Chinese Chemical Letters 36 (2025) 110251

Contents lists available at ScienceDirect

Chinese Chemical Letters

journal homepage: www.elsevier.com/locate/cclet

Kidney targeted delivery of siRNA mediated by peptide-siRNA conjugate for the treatment of acute kidney injury

Mengmeng Yuan[b,d,1], Xiwen Hu[a,b,1], Na Li[c,1], Limin Xu[b], Mengxi Zhu[b], Xing Pei[e], Rui Li[b], Lu Sun[b], Yupeng Chen[c], Fei Yu[b], Huining He[a,b,*]

[a] International Joint Laboratory of Ocular Diseases, School of Biomedical Engineering and Technology, Tianjin Medical University, Tianjin 300070, China
[b] Tianjin Key Laboratory on Technologies Enabling Development of Clinical Therapeutics and Diagnostics, School of Pharmacy, Tianjin Medical University, Tianjin 300070, China
[c] Key Laboratory of Immune Microenvironment and Disease (Ministry of Education), The Province and Ministry Co-sponsored Collaborative Innovation Center for Medical Epigenetics, Department of Biochemistry and Molecular Biology, School of Basic Medical Sciences, Tianjin Institute of Urology, The Second Hospital of Tianjin Medical University, Tianjin Medical University, Tianjin 300070, China
[d] Department of Pharmacy, Affiliated Hospital of Shandong Second Medical University, Weifang 261031, China
[e] Tianjin Key Laboratory of Food and Biotechnology, School of Biotechnology and Food Science, Tianjin University of Commerce, Tianjin 300134, China

ARTICLE INFO

Article history:
Received 16 May 2024
Revised 11 July 2024
Accepted 15 July 2024
Available online 15 July 2024

Keywords:
siRNA delivery
Kidney target
Targeting peptide
Conjugate
Acute kidney injury

ABSTRACT

Small interfering RNA (siRNA), a promising revolutionary therapy, faces delivery obstacles due to its poor targeting, strong charge negativity and macromolecular nature. Clinical-approved siRNAs can now only be delivered to the liver mediated by the chemically conjugated *N*-acetylgalactosamine (GalNAc) ligand, the conjugate can be effectively uptaken into cells through interaction with asialoglycoprotein receptor (ASGPR) highly expressed on liver hepatocytes. To further explore an efficient non-hepatic targeted delivery strategy, in this study, we designed a delivery system that chemically conjugated p53 siRNA to renal tubular cell-targeting peptides for targeting the kidney, which was suitable for industrial transformation. Results showed that peptide-siRNA conjugate could specifically enter renal tubular epithelial cells and silence target genes. In cisplatin-induced acute kidney injury (AKI) mice, peptide-siRNA conjugate blocked the p53-mediated apoptotic pathway and alleviated renal damage. The innovative proposed system to conjugate kidney-targeting peptides with siRNA achieved the efficient kidney-targeted delivery of siRNA and provided a prospective choice for treating AKI.

siRNA therapy, which reduces the expression of target genes by degrading target mRNAs in the cytoplasm [1,2], has become a promising novel investigational medication due to its high specificity in treating various diseases in recent years [3,4]. However, the difficulties of siRNA delivery have been a severe obstacle in its therapeutic applications due to its negative charge, high molecular weight, poor membrane permeability and the instability of unmodified siRNA in the bloodstream [5,6]. Therefore, various synthetic nanocarriers including lipid nanoparticles [7,8], polymer nanoparticles [9], dendronized polymer [10], ligand-conjugated nanoparticles [11] and biomimetic nanoparticles of cell membranes [12] have been employed to deliver siRNA to target cells and to obtain effective therapeutic outcomes. siRNA delivery can be realized by loading siRNA onto the surface of the carrier, coassembling with the nanocarrier or directly encapsulating siRNA inside the carrier. Although synthetic nanocarriers have been widely studied due to their convenient preparation and high yield, the issues of synthetic materials-induced immune response, potential toxicity and non-specific targeting cannot be ignored [13].

Chemical conjugate technology is a promising siRNA delivery strategy, in which various ligands including small molecule drugs, peptides, antibodies, and aptamers are covalently conjugated to siRNA to improve cell uptake and target specific cell types [14]. The ligand-based siRNA conjugate to achieve nucleic acid drug-specific targeted delivery and their penetration or retention at the disease site is still the main formulation used in the clinic [15]. Five of the six clinical-approved siRNA drugs all apply GalNAc-siRNA chemical conjugate technology to achieve liver-targeted delivery [16]. The delivery strategy is based on the high-affinity binding of *N*-acetylgalactosamine (GalNAc) to the asialoglycoprotein receptor (ASGPR) [17-19], which is abundantly expressed on the surface of hepatocytes. With continuous efforts, extrahepatic siRNA conjugate

* Corresponding author.
E-mail address: hehuining@tmu.edu.cn (H. He).
[1] These authors contributed equally to this work.

https://doi.org/10.1016/j.cclet.2024.110251
1001-8417/

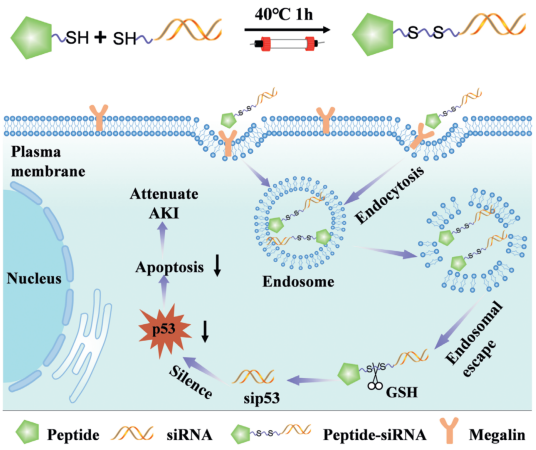

Fig. 1. Schematic representation of the mechanism of renal targeted delivery of siRNA. Peptide-siRNA conjugate could efficiently target renal tubular epithelial cells and be internalized, increasing the siRNA enrichment within the kidney.

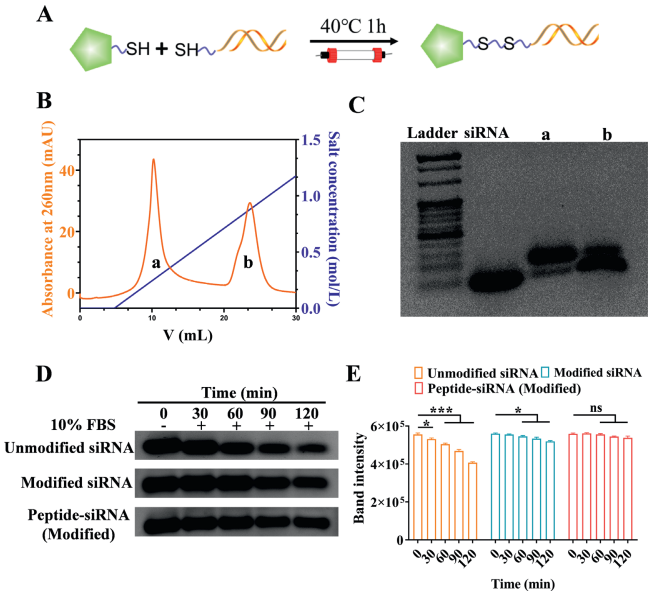

Fig. 2. Characterization and serum stability evaluation of the peptide-siRNA conjugate. (A) The synthesis of peptide-siRNA conjugate. (B) Purification of the peptide-siRNA conjugate through DEAE column (a: peptide-siRNA conjugate; b: siRNA-siRNA). (C) The 2% agarose gel electrophoresis was used to identify the peptide-siRNA conjugate (a: peptide-siRNA conjugate; b: siRNA-siRNA). (D) Agarose gel electrophoresis of peptide-siRNA (modified) after incubation with 10% FBS for indicated times. (E) Quantification of band intensity of different groups after incubation with 10% FBS for indicated times. Data are presented as mean ± SEM ($n = 3$ per group). ns, no significance. $^{*}P < 0.05$, $^{***}P < 0.001$ *vs.* unmodified siRNA group.

delivery platforms have also been explored, Liu and co-workers successfully delivered siRNA to tumors through covalently conjugated cyclo(cRGD) peptides [20]. However, the delivery of siRNA by chemical conjugate technology to kidney has been explored to a very limited extent.

Acute kidney injury (AKI), a common clinical complication with 10%–15% occurrence in inpatients and over 50% occurrence in intensive care [21,22], is featured by sudden renal dysfunction or impairment characterized by reduced glomerular filtration rate, increased serum urea nitrogen and creatinine concentrations, reduced or absent urine output [23-25]. The multiple and complicated pathophysiological mechanisms of AKI, including ischemia-reperfusion, nephrotoxic drugs, sepsis, *etc.* [26], resulted in the lack of specific pharmacological treatment in clinical practice to prevent the evolution of the injury or reverse it. Several nanomedicines are already developed for treating acute kidney injury [27]. Nie *et al.* prepared nanoparticles (PUA NPs@RES) with PUA as a bioactive nanocarrier and resveratrol (RES) as a model drug, which significantly improved drug accumulation in the kidneys and showed good biocompatibility [28]. Despite the advancements in nanomedicine, which have primarily focused on anti-inflammatory and antioxidative therapies for acute kidney injury (AKI), gene therapies targeting AKI have not been extensively explored. The tumor suppressor p53 is known to be upregulated in renal tubular epithelial cells, playing a crucial role in the onset and subsequent renal repair of AKI by primarily regulating cell cycle arrest, apoptosis, and autophagy [29-31]. Studies showed that inhibition of p53 by pifithrin-α, an inhibitor of p53, or dominant-negative mutant p53 could dramatically attenuate the renal tubular epithelial cell injury and apoptosis [32,33]. Hence, inhibition of p53 expression by sequence-specific siRNA might be a viable therapy method for AKI.

In this work, we designed a kidney-targeted peptide-siRNA conjugate delivery system for targeting renal tubular epithelial cells, silencing p53 expression and treating acute kidney injury (Fig. 1). The results demonstrated that the peptide-siRNA conjugate could effectively target to renal tubular epithelial cells and be internalized through the receptor macroprotein and showed a marked ability to knock down genes *in vitro* and *in vivo*. More importantly, peptide-siRNA conjugate exhibited better anti-apoptotic effect in acute kidney injury model compared with the Lipo/siRNA. This study presents novel strategy for siRNA delivery to the kidney and enhances therapeutic efficacy against AKI.

To achieve the efficient renal targeting delivery of siRNA, a peptide with the sequence $(KKEEE)_3$ K was selected as targeting ligand that could specifically interact with macroprotein expressed on renal tubular cells for efficient renal targeting. One study found that the peptide sequence $(KKEEE)_3$ K triggered abnormal renal specificity when at elevated accumulation rates [28]. We introduced cysteine into the peptide so that the final sequence of the targeting peptide was C$(KKEEE)_3$ K, then the renal tubular targeting peptide was chemically conjugated to siRNA *via* disulfide bond as shown in Fig. 2A. The disulfide linkage could be cleaved under the reducing cytoplasmic environment to release free siRNA duplexes. DEAE column was employed to separate the components after the reaction. The components with different charges possessed different binding abilities with the DEAE column. The peptide-siRNA conjugate (a) and by-product siRNA-siRNA (b) with different levels of binding affinity bound to the DEAE column were then eluted using NaCl solutions of different gradients. As shown in Fig. 2B, at NaCl concentration of 0.2 mol/L, peptide-siRNA conjugate was eluted from the DEAE column, while the much more negatively charged siRNA-siRNA was eluted at 0.65 mol/L NaCl with a delayed peak emergence. As shown in Fig. S1 (Supporting information), the yield of the peptide-siRNA conjugate was approximately 58.78% by quantifying the peak area and using the following formula: $\text{Yield}_{\text{siRNA}} = A_{\text{conjugate}}/(A_{\text{conjugate}} + A_{(\text{siRNA-siRNA})}) \times 100\%$.

Ensuring the successful preparation of peptide-siRNA conjugate is a key premise for siRNA to silence the target gene, the collected fractions were analyzed by agarose gel electrophoresis. As shown in Fig. 2C, compared with siRNA monomer, peptide-siRNA conjugate exhibited a lagging band due to the effect of the peptide on the molecular weight and spatial structure of siRNA, resulting in the change of the migration rate of the siRNA band. However, the band of by-products siRNA-siRNA, the siRNA dimer with a molecular weight of about 42 bp, appeared near 40 bp indicated by the ladder, which was consistent with the findings of the agarose gel electrophoresis. All results suggested the successful synthesis of the peptide-siRNA conjugate.

Naked siRNA is easily degraded when it reaches the target site through blood circulation, we thereby selected chemically modified siRNA to synthesize peptide-siRNA conjugate. All the components were incubated with 10% fetal bovine serum (FBS) at different time points to evaluate the stability after modification. As shown in Fig. 2D, the degradation of the unmodified siRNA was apparent with the prolongation of incubation time. However, modified siRNA and synthesized peptide-siRNA conjugate were only slightly degraded during up to two hours of serum exposure. Quantitative results in Fig. 2E clearly showed the variation of siRNA bands in each group. These results indicated that the stability of siRNA was improved after chemically stable modification and supported further application of conjugate *in vivo*.

The primary renal tubular epithelial cells (PTC) were isolated by the magnetic bead method to precisely confirm the biological effects *in vitro*. Cellular markers were observed by immunofluorescence before and after magnetic bead isolation, respectively. As shown in Fig. S2 (Supporting information), before magnetic bead separation, the mixture contained tubules and the glomerulus and the result showed double positive (synaptopodin-red labeled glomerulus, lotus tetragonolobus lectin (LTL)-green labeled tubules). After separation by magnetic beads, glomerulus that trapped magnetic beads were adsorbed to the tube wall by the magnetic holder, leaving the tubules at the bottom of the tube and showing single positive tubules. After passaging and amplification, the obtained renal tubular epithelial cells were used for subsequent experiments.

To demonstrate whether the selected targeting peptide could bind to the renal tubular epithelial cell-specific expression of macroproteins and mediate endocytosis, the fluorescein isothiocyanate (FITC)-labeled targeting peptides were directly co-incubated with primary renal tubular epithelial cells (PTC) and negative control renal medullary collecting duct 3 epithelial cells (IMCD3) that did not express macroprotein, and the targeting effect was explored by intracellular uptake of the targeting peptides. As shown in Fig. S3 (Supporting information), the green fluorescence could be detected at the low concentration of 1 μmol/L in PTC cells, and the fluorescence intensity was increased with concentration of the targeting peptide, whereas no green fluorescence was evident in IMCD3 cells even at high concentrations. Based on the comparison between the two cells, the results preliminarily revealed that targeting peptides can specifically target renal tubular epithelial cells and be internalized.

In vitro, the toxicity of peptide-siRNA conjugate on renal tubular epithelial cells was investigated by cell counting kit-8 (CCK-8) method, and Lipofectamine 2000, the commonly used transfection reagent for siRNA was used as control. We have measured the cytotoxicity of peptide-siRNA conjugate and Lipofectamine 2000 in PTC cells at siRNA concentrations ranging from 50 nmol/L to 200 nmol/L. According to Fig. S4 (Supporting information), the results showed that the conjugate was safe up to 200 nmol/L siRNA concentration, with cell viability greater than 85%. Conversely, when the cells were treated with Lipofectamine 2000, elevated cytotoxicity was observed at 200 nmol/L siRNA with increasing concentrations. Furthermore, cell viability was reduced by approximately 50% at 200 nmol/L siRNA. The results of CCK-8 detection of cytotoxicity demonstrated that the prepared conjugate had a low impact on cells and provided optimum security compared with the transfection reagent. However, Lipofectamine 2000 had a favorable transfection effect, its toxicity should not be ignored.

We further investigated the mechanism of cellular uptake of peptide-siRNA conjugate by blocking the macroprotein receptor. As shown in Fig. 3A, significant red fluorescence can be viewed after direct incubation of peptide-siRNA conjugate with PTC cells. On the contrary, when the cells were pre-treated with peptide before being incubated with peptide-siRNA conjugate, the red fluorescence of Cy5-labeled siRNA was significantly reduced. Quantitative analysis of the fluorescence intensity in Fig. 3B revealed that the preincubated group (peptide+peptide-siRNA) had only about a third of the fluorescence intensity of the untreated group (peptide-siRNA), which indicated that these differences in outcome may be due to macroprotein-mediated endocytosis and demonstrated that peptide-siRNA conjugate was mediated into cells by targeting peptides.

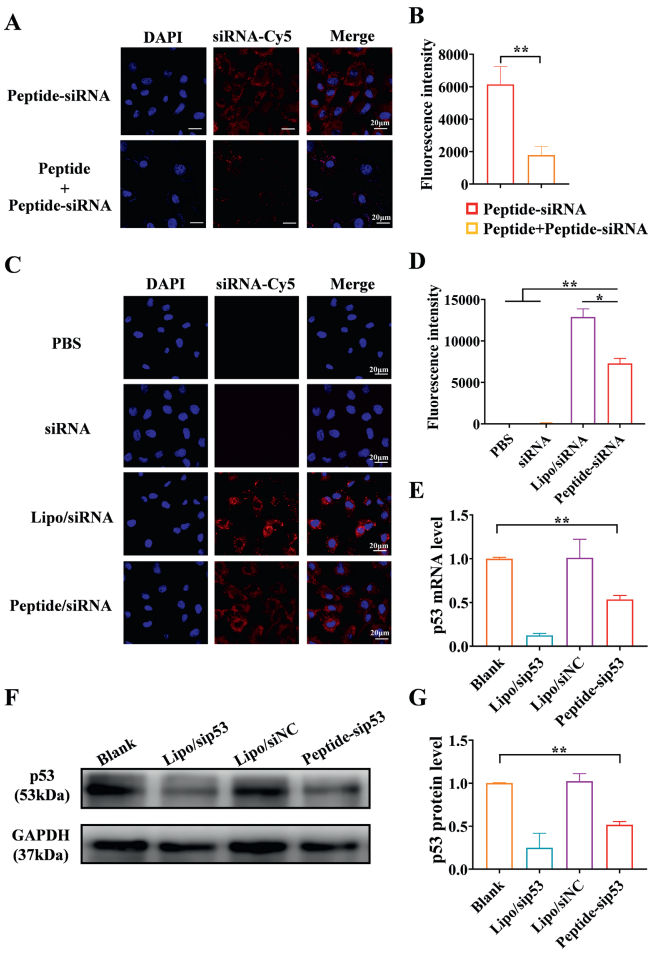

Fig. 3. Cellular uptake and gene silencing efficacy of peptide-siRNA conjugate *in vitro*. (A) Representative confocal microscopy images of peptide-siRNA conjugate cellular uptake mechanism (nuclei-blue, siRNA-red). (B) Quantification of cellular uptake for (A). (C) Representative confocal microscopy observation of PTC cells treated with PBS, siRNA, Lipo/siRNA, and peptide-siRNA conjugate (nuclei-blue, siRNA-red). (D) Quantification of cellular uptake for (C). (E) p53 mRNA levels were detected by qRT-PCR. (F) p53 protein levels were detected by Western blot. GAPDH, glyceraldehyde-3-phosphate dehydrogenase. (G) Quantitative analysis of p53 protein expression. Data are presented as mean ± SEM ($n = 3$ per group). $^{*}P < 0.05$, $^{**}P < 0.01$. Scale bar: 20 μm.

To visualize the cellular uptake of siRNA, fluorescence patterns were examined using confocal laser scanning microscopy. Four samples were prepared and examined: (1) PBS, (2) free siRNA, (3) Lipofectamine 2000/siRNA, and (4) peptide-siRNA conjugate. Lipofectamine 2000, the commercially available transfection reagent commonly used for siRNA, served as positive control. As depicted in Figs. 3C and D, confocal images showed minimal cellular uptake of free siRNA, which was consistent with the PBS group. On the other hand, both Lipofectamine 2000/siRNA and peptide-siRNA conjugate treatments exhibited strong fluorescence intensity within the cells. The merged image of the conjugate further implied that the majority of the conjugate was located in the cyto-

plasm. In our previous studies, we used two different compounds connected by either a non-cleavable maleimide-sulfide bond or a cytosol-cleavable disulfide bond to investigate their localization in cells. Confocal images revealed that the fluorescence of conjugate containing disulfide bond resided predominantly in the cytoplasmic region, while the non-reducible compound covered the entire cell with fluorescence, suggesting chemical reduction quickly broke the disulfide link in the cytosol and allowing the released siRNA to remain in the cytosolic compartment [34]. These results indicated that the conjugate strategy efficiently achieved cytoplasm delivery of siRNA. Although the intracellular uptake of Lipofectamine 2000 was superior to that of the conjugate *in vitro*, the reagent lacked specificity and safety, thus limiting the application for delivering siRNA to specific organs or cells *in vivo*.

The lysosome escape of peptide-siRNA conjugate is crucial for efficient gene silencing. Hence, the siRNA labeled with Cy5 was conjugated with the peptide and incubated with the cells for specific time. Subsequently, intracellular lysosomes were labeled with a lysotracker, and colocalization was observed using confocal microscopy. As shown in Fig. S5 (Supporting information), there was no obvious colocalization between peptide-siRNA conjugate and lysosomes. The Mander's coefficient between lysosome and siRNA was 0.281, as analyzed using ImageJ software. The results showed that the peptide-siRNA conjugate was not captured by lysosomes after being taken up by cells, which laid a foundation for the successful entry of the conjugate into the cytoplasm to facilitate gene silencing.

The gene silencing efficacy of peptide-siRNA conjugate was examined by qRT-PCR and Western blot analysis. As shown in Fig. 3E, while the knockdown effect of lipo/sip53 was more apparent compared to the blank and lipo/siNC control, the expression of p53 mRNA was dramatically downregulated by 50% after treatment with peptide-siRNA conjugate. Similarly, the results shown in Figs. 3F and G indicated that p53 in protein level was also significantly reduced by 50% after treatment with peptide-siRNA conjugate, compared to the control group. The gene silencing effect of Lipofectamine 2000 was consistent with the cellular uptake effect, which was superior to that of the conjugate *in vitro*. However, Lipofectamine 2000 was not targeted in subsequent *in vivo* experiments. In conclusion, the results confirmed that peptide-siRNA conjugate was a reliable method for delivering functional sip53 into PTC cells, reducing the expression level of p53 and achieving good gene silencing effect.

A necessary condition for effective therapy is the adequate accumulation of therapeutic medicines in their target tissues. While free siRNA shows natural nephrogenicity, it is rapidly metabolized and eliminated *in vivo* and does not effectively enter renal tubular epithelial cells. Therefore, it is crucial to ascertain the distribution of peptide-siRNA conjugate *in vivo* before exploring its therapeutic potential. All animal experiments were conducted in accordance with the National Institutes of Health's guidelines for the use and care of laboratory animals, and were carried out in compliance with the authorized protocols of the animal welfare and Ethics Committee of Tianjin Medical University.

Following intravenous injections of Cy5-labeled peptide-siRNA conjugate and free siRNA-Cy5, the biodistribution was respectively evaluated after 12 and 36 h. As shown in Figs. 4A and B, there was a small amount of accumulation in the kidney after injection in the free siRNA group, and the fluorescence intensity decreased with time, because the siRNA itself had some nephrogenic, and the instability made it extremely easy to degrade in the kidneys. In contrast, substantially more accumulation in the kidneys was observed post-injection when the siRNA was administered as peptide-siRNA conjugate. *Ex vivo* imaging data for major organs, as shown in Fig. S6 (Supporting information), indicated that peptide-siRNA conjugate had more accumulation in the kidney compared with the

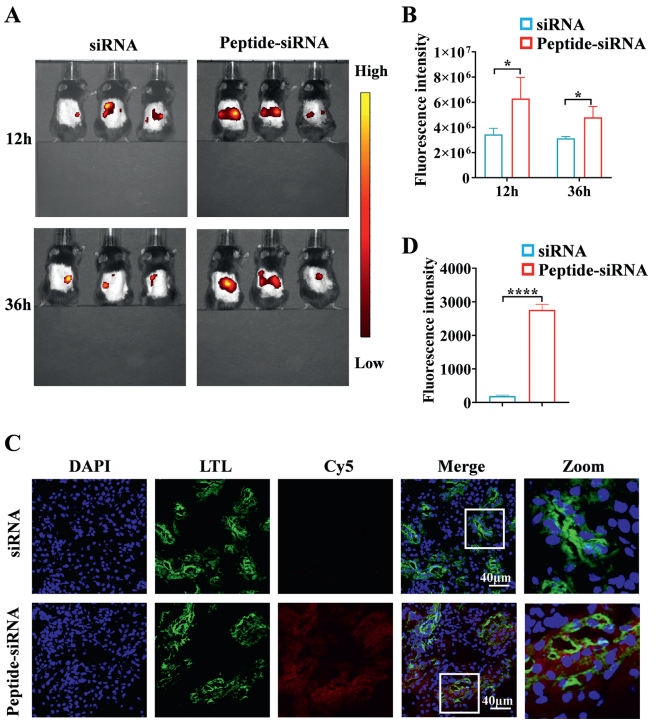

Fig. 4. Distribution of peptide-siRNA conjugate *in vivo*. (A) Biodistribution imaging of free siRNA-Cy5 and peptide-siRNA-Cy5 at 12 and 36 h *in vivo*. (B) Quantification of fluorescence intensity at 12 and 36 h by the Living Image software. (C) Representative confocal images of kidney sections 36 h after intravenous injection of peptide-siRNA conjugate (nuclei-blue, siRNA-red, LTL-green). Scale bar: 40 μm. (D) Quantification of fluorescence intensity of kidney sections. Data are presented as mean ± SEM ($n = 3$ per group). $^{*}P < 0.05$, $^{****}P < 0.0001$.

free siRNA and Lipo/siRNA groups at 12 h after injection. To further investigate the distribution site of peptide-siRNA conjugate, confocal microscopy was applied to observe the fluorescence distribution of frozen kidney sections. The renal tubules were labeled with FITC-labeled LTL, and the colocalization of siRNA-Cy5 red fluorescence and LTL green fluorescence was observed. As shown in Fig. 4C, the results showed that there was no obvious red fluorescence in the free siRNA group, but red fluorescence could be seen in the peptide-siRNA conjugate group and distributed around the nucleus. More importantly, the red fluorescence of peptide-siRNA was only found in LTL-labeled renal tubule areas with no red fluorescence in other regions, which indicated that the peptide-siRNA conjugates had excellent renal tubule targeting ability. In Fig. 4D, the fluorescence intensity of the peptide-siRNA conjugate was nearly 13-fold higher than that of free siRNA. Overall, the colocalization of the two fluorescence signals suggested that peptide-siRNA conjugate had preferential renal targeting ability *in vivo* and could target renal tubular epithelial cells for absorption.

Cisplatin (CDDP), one of the most widely used and successful anti-cancer drugs, is used alone or in combination for the treatment of most cancers, but its application is limited by nephrotoxicity, with an incidence of AKI of approximately 38% in patients treated with cisplatin [35,36]. AKI is a common clinical complication with a predictable pathogenesis, which progresses rapidly once it occurs. Thus, we chose cisplatin-induced AKI to construct an experimental model in animals and applied an early intervention approach to prevent the development of AKI, the detailed animal program is shown in Fig. 5A. We initially evaluated the therapeutic efficacy of the peptide-siRNA conjugate by measuring blood urea nitrogen (BUN) and serum creatinine (SCr), which were two important indicators for assessing kidney function. Based on the results shown in Figs. 5B and C, following cisplatin-induced AKI

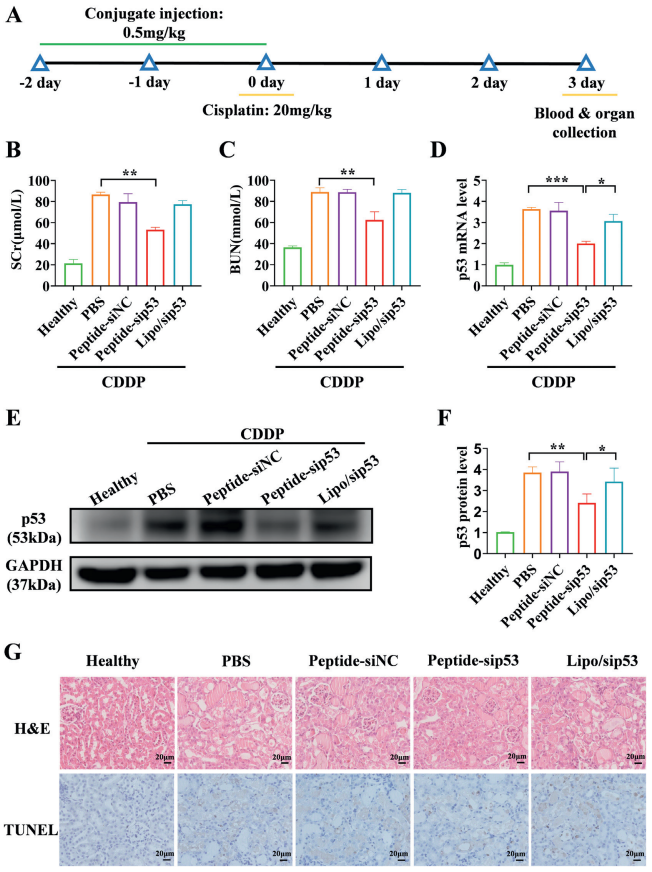

Fig. 5. Therapeutic and gene silencing efficacy of peptide-siRNA conjugate in cisplatin (CDDP)-induced AKI *in vivo*. (A) Animal experimental design and treatment protocol. (B) Serum creatinine (SCr) and (C) blood urea nitrogen (BUN) level after treatment. (D) Renal p53 mRNA levels were detected by qRT-PCR. (E) Renal p53 protein levels were detected by Western blot. (F) Quantitative analysis of p53 protein expression. (G) H&E and TUNEL staining were used to analyze the histopathological status and apoptosis of renal tissue respectively. Scale bar: 20 μm. Data are presented as mean ± SEM ($n = 6$ per group). $^{*}P < 0.05$, $^{**}P < 0.01$, $^{***}P < 0.001$.

in mice, the BUN and SCr levels in the PBS group significantly increased compared to the healthy group. The levels of BUN and SCr decreased in the mice pretreated with peptide-sip53 conjugate, the Lipo/sip53 group did not reduce BUN and SCr due to the lack of *in vivo* targeting, and the above results demonstrated that peptide-sip53 conjugate could protect renal function and somewhat mitigate renal damage.

We evaluated the gene-silencing effect of peptide-siRNA conjugate by qRT-PCR and Western blot at mRNA and protein levels *in vivo*. As shown in Figs. 5D–F, the expression level of p53 was increased after the mice developed AKI induced by cisplatin. The p53 gene was silenced in advance after administration with peptide-sip53 conjugate, which could prevent the up-regulation of p53 during the development of AKI and intervene the occurrence of AKI. When compared with the PBS group, the peptide-sip53 conjugate treatment caused nearly 45% silencing of the p53 protein and mRNA levels. Furthermore, although Lipofectamine 2000 has eminent gene silencing effect *in vitro*, owing to the absence of *in vivo* targeting, it does not exhibit good gene silencing effect.

The therapeutic effect of the peptide-sip53 conjugate was further evaluated through histological analysis of the kidney sections. As shown in Fig. 5G, hematoxylin and eosin (H&E) staining showed normal renal morphology with the brush-like margin of the renal tubules observed in the healthy group. However, the renal tubules showed obvious structural damage, such as cavitation and disappearance of brush border in cisplatin-induced AKI. Neither the peptide-siNC group nor the Lipo/sip53 group showed significant improvement in renal function, which was attributed to the lack of targeting *in vivo*. The formation of cavitation was significantly reduced in the peptide-sip53 treatment group compared to the other groups. Terminal deoxynucleotidyl transferase mediated dUTP nick-end labeling (TUNEL) staining showed that the nuclei of kidney cells in the healthy group were intact and clear, with almost no apoptotic cells. In contrast, the number of apoptotic cells in the kidneys of mice with AKI induced by cisplatin was significantly increased. Compared to the other treatment groups, the peptide-sip53 conjugate treatment reduced the percentage of positive apoptotic cells in renal tissue, indicating the potent anti-apoptotic properties of the conjugate. The results suggested that peptide-sip53 conjugate could alleviate the renal injury of AKI mice and improve renal function.

Finally, we evaluated the safety of the peptide-sip53 conjugates *in vivo*. H&E staining of major organ sections investigated whether the peptide-sip53 conjugate strategy negatively affected organs other than the kidney. As shown in Fig. S7 (Supporting information), there was no severe injury to the heart, liver, spleen, and lung. Additionally, no significant tissue injury or pathological changes were observed in the peptide-sip53 group compared to the PBS group, indicating that the toxic and side effects of the peptide-sip53 conjugate on other organs were minimal, demonstrating favorable biosafety in living organisms. These results confirmed the biocompatibility of the peptide-sip53 conjugate and suggested its potential in treating AKI.

siRNA is a promising tool for treating multiple illnesses by focusing on disease-related genes. Five of the six clinically approved siRNA drugs all apply GalNAc-siRNA chemical conjugate technology to achieve liver-targeted delivery. Although there have been many studies on extrahepatic targeted drug delivery, no significant breakthrough has been achieved. In this study, we successfully achieved kidney-targeted siRNA delivery by developing a peptide-siRNA conjugate delivery system. We have demonstrated that renal tubular epithelial cells can efficiently take up the peptide-siRNA conjugate and subsequently implement effective p53 gene silencing at the cellular level. Furthermore, the peptide-siRNA conjugate demonstrated significant accumulation within the kidney and exhibited promising therapeutic efficacy by inhibiting the p53-mediated apoptotic pathway in the context of cisplatin-induced acute kidney injury. This research offers a novel approach to targeted siRNA delivery to the kidney and holds promise for broadening the clinical utility of siRNA as a potential therapeutic strategy for AKI.

Declaration of competing interest

The authors declare that they have no known competing financial interests or personal relationships that could have appeared to influence the work reported in this paper.

CRediT authorship contribution statement

Mengmeng Yuan: Writing – original draft, Software, Methodology, Investigation, Data curation. **Xiwen Hu:** Writing – original draft, Validation, Investigation, Data curation. **Na Li:** Validation, Investigation. **Limin Xu:** Validation, Investigation. **Mengxi Zhu:** Validation, Investigation. **Xing Pei:** Investigation. **Rui Li:** Investigation. **Lu Sun:** Conceptualization. **Yupeng Chen:** Supervision, Resources. **Fei Yu:** Formal analysis. **Huining He:** Writing – review & editing, Funding acquisition, Conceptualization.

Acknowledgments

This work was supported by the National Key Technologies Research and Development Plan (No. 2021YFE0106900), the National Natural Science Foundation of China (No. 82173769), the Basic Research Cooperation Project of Beijing, Tianjin, Hebei from the Natural Science Foundation of Tianjin (No. 20JCZXJC00070), and the Applied Basic Research Multi-investment Foundation of Tianjin (No. 21JCYBJC01540).

Supplementary materials

Supplementary material associated with this article can be found, in the online version, at doi:10.1016/j.cclet.2024.110251.

References

[1] W. Alshaer, H. Zureigat, A. Al. Karaki, et al., Eur. J. Pharmacol. 905 (2021) 174178.
[2] Q. Wang, Q. Jiang, D. Li, et al., Chin. Chem. Lett. 35 (2024) 108683.
[3] M.L. Bobbin, J.J. Rossi, Annu. Rev. Pharmacol. Toxicol. 56 (2016) 103–122.
[4] H. Zogg, R. Singh, S. Ro, Int. J. Mol. Sci. 23 (5) (2022) 2736.
[5] Y. Dong, D.J. Siegwart, D.G. Anderson, Adv. Drug Deliv. Rev. 144 (2019) 133–147.
[6] J. Wang, Z. Lu, M.G. Wientjes, J.L. Au, AAPS J. 12 (4) (2010) 492–503.
[7] L. Zhang, Z. Dong, S. Yu, et al., Chin. Chem. Lett. 35 (2024) 109101.
[8] W. Cao, X. Zhang, R. Li, et al., J. Control. Release 368 (2024) 52–65.
[9] W. Tang, S. Panja, C.M. Jogdeo, et al., Biomaterials 285 (2022) 121562.
[10] J. Chen, H. Zhu, J. Xia, et al., Adv. Sci. 10 (2023) e2206306.
[11] Q. Qin, M. Wang, Y. Zou, et al., MedComm Biomater. Appl. 2 (2023) e65.
[12] Y. Wang, C. Zhang, S. Han, et al., Chin. Chem. Lett. 35 (2024) 109578.
[13] M. Moazzam, M. Zhang, A. Hussain, et al., Mol. Ther. 32 (2024) 284–312.
[14] J.W. Lee, J. Choi, Y. Choi, et al., J. Control. Release 351 (2022) 713–726.
[15] R. Liu, C. Luo, Z. Pang, et al., Chin. Chem. Lett. 34 (2023) 107518.
[16] A. Maguregui, H. Abe, ChemBioChem 21 (2020) 1808–1815.
[17] A.D. Springer, S.F. Dowdy, Nucleic Acid Ther. 28 (2018) 109–118.
[18] K.G. Rajeev, J.K. Nair, M. Jayaraman, et al., ChemBioChem 16 (2015) 903–908.
[19] B. Hu, S. Kong, Y. Weng, et al., Chin. Chem. Lett. 34 (2023) 108210.
[20] X. Liu, W. Wang, D. Samarsky, et al., Nucleic Acids Res. 42 (2014) 11805–11817.
[21] S.R. Gonsalez, A.L. Cortês, R.C.D. Silva, et al., Pharmacol. Ther. 200 (2019) 1–12.
[22] C. Ronco, R. Bellomo, J.A. Kellum, Lancet 394 (2019) 1949–1964.
[23] A. Vijayan, Nat. Rev. Nephrol. 17 (2021) 87–88.
[24] E.A.J. Hoste, J.A. Kellum, N.M. Selby, et al., Nat. Rev. Nephrol. 14 (2018) 607–625.
[25] J.A. Kellum, J.R. Prowle, Nat. Rev. Nephrol. 14 (2018) 217–230.
[26] R.L. Mehta, E.A. Burdmann, J. Cerdá, et al., Lancet 387 (2016) 2017–2025.
[27] Y. Nie, L. Wang, X. You, et al., J. Nanobiotechnol. 20 (2022) 505.
[28] Y. Nie, L. Wang, S. Liu, et al., J. Nanobiotechnol. 22 (2024) 84.
[29] C. Tang, Z. Ma, J. Zhu, et al., Pharmacol. Ther. 195 (2019) 5–12.
[30] A. Wischnjow, D. Sarko, M. Janzer, et al., Bioconjug. Chem. 27 (2016) 1050–1057.
[31] H.F. Horn, K.H. Vousden, Oncogene 26 (2007) 1306–1316.
[32] Y.L. Shen, L. Sun, Y.J. Hu, et al., Am. J. Transl. Res. 8 (2016) 4040–4053.
[33] M. Jiang, X. Yi, S. Hsu, et al., Am. J. Physiol. Renal Physiol. 287 (2004) F1140–F1147.
[34] J. Ye, E. Liu, J. Gong, et al., Theranostics 7 (2017) 2495–2508.
[35] S. Ghosh, Bioorg. Chem. 88 (2019) 102925.
[36] S.M. Sears, L.J. Siskind, J. Am. Soc. Nephrol. 32 (2021) 1559–1567.